UNIVERSITY OF CALIFORNIA
RIVERSIDE

Stellar Variability of Known Hosts Observed by TESS

A Thesis submitted in partial satisfaction
of the requirements for the degree of

Master of Science

in

Earth and Planetary Sciences

by

Emilie R. Simpson

June 2022

Thesis Committee:

Professor Stephen Kane, Chairperson
Professor Edward Schwieterman
Professor Gabriela Canalizo

The Thesis of Emilie R. Simpson is approved:

Chairperson

University of California, Riverside

Acknowledgments

I am grateful to my advisor, without whose help, I would not have been here.

To my family, for all their love and support.

ABSTRACT OF THE THESIS

Stellar Variability of Known Hosts Observed by TESS

by

Emilie R. Simpson

Master of Science, Graduate Program in Earth and Planetary Sciences
University of California, Riverside, June 2022
Professor Stephen Kane, Chairperson
Professor Edward Schwieterman

As long as astronomers have searched for exoplanets, the intrinsic variability of host stars has interfered with the ability to reliably detect and confirm exoplanets. In this thesis, I will give an overview of how stellar variability affects the way astronomer's perceive planets as well as how they affect their planets directly. I first present the results of a photometric data analysis for the known planet hosting star, BD-06 1339, observed by the Transiting Exoplanet Survey Satellite (TESS) during Sector 6 at 2 minute cadence. I discuss evidence that suggests the observed 3.9 day periodic radial velocity signature may be caused by stellar activity rather than a planetary companion, since variability detected in the photometric data are consistent with the periodic signal. I will then conduct a population study of known hosts observed by TESS and discuss both correlations and unique targets that call these variable stars their home.

Contents

List of Figures

List of Tables

Chapter 1

Introduction

Exoplanetary science has been pivotal in discovering how our own planet was formed and evolved, and how unique our system is among other planetary systems. WHile Earth is the baseline for the study of planetary habitability and the evolution of life, this thesis will focus on the identity and consequences of host stars.

Stars come in a broad range of sizes, temperatures, and compositions. While many types of stars can be hosts to exoplanets, certain characteristics can affect the conditions of those exoplanets. If the planet is too close to a star, its atmosphere can suffer from inflation or be stripped entirely from the planet. This presents the issue of being able to properly sustain habitability. The distance and orbital relationship of the exoplanet and the host star can affect its Habitable Zone (Kopparapu et al. 2013, 2014).

1.1 Exoplanets History

Exoplanets have made their impact on the field of observational astronomy long before they were recognized as the source of unexpected results. Speculation to their existence was supported by planet formation models that were developed before their discovery.

The first exoplanet to be found was in 1913, but was not identified by any traditional methods of exoplanet detection known and utilized today. Rather, it was the result of a stellar observing team taking spectroscopic data of ground-observable stars. The original plate of van Maanen's Star was taken from Mount Wilson and it was unidentified due to the anomalous spectral lines associated with the star. It wouldn't be until 2014 when Ben Zuckerman was able to identify the odd spectral lines: calcium ions, a telltale residual sign of an exoplanet (Zuckerman 2015) that had been destroyed by its star. While the connection would not be made for almost a century, the planet's effect on the perception of the host star would prove to be the basis of exoplanet detection methods.

Since then, exoplanets have solidified their reputation among the field of astronomy, as well as other fields of astrobiology, as both a solution to the mysteries surrounding our own Earth and as a way of determining the probability of life beyond our own system. In popular media, exoplanets have been the topic of conversation as glimpses into entire new worlds and cultures, alluding to how they might mirror our own progress, conflicts, and triumphs. It is the focus of this thesis to determine how these worlds may be affected by their stars, and which cases lend to the habitability of their planets.

1.2 Detection Methods of Exoplanets

Exoplanet detection began very suddenly in the 1990s, when the first exoplanet was detected via radial velocity signatures (Mayor & Queloz 1995). The methods necessary to find exoplanets had previously been technically feasible (Black 1980; Bracewell & MacPhie 1979; Kenknight 1977). It became apparent that discovering such dim and proportionally small bodies required technology and methods that would rely on these features for successful detection. With time came new methods, and with new methods came new classes and types of exoplanets that would have otherwise escaped discovery entirely. Holes still exist within our overall population of found and confirmed exoplanets, raising questions about exoplanet formation: the radius gap (Fulton et al. 2017) between super earths and sub-Neptunes is a great example of this. In this gap, what dictates the survival of terrestrial planets of a certain size? Also, if planetary bodies of this size are particularly rare, would the star be responsible for determining the physical state of these bodies? We hope that with future missions, as well as continued research of exoplanets that we have found, that these questions will eventually be answered.

I will now discuss the primary methods of detection that these targets were discovered or confirmed by. I will discuss the radial velocity and transit methods primarily, since they are responsible for the discovery of most planets. All planetary data mentioned here have been sourced by the NASA Exoplanet Archive.

1.2.1 Radial Velocity

A planet will orbit its star within the confines of the host's gravitational influence. The star, depending on the size of the orbiting body, will also have its own orbit along a centric point of the system due to the gravitational pull of the planet. As the star shifts back and forth within a single planetary orbit, the spectral lines of the star (as observed from Earth) also shift. This blueshift and redshift we observe reveals the presence of exoplanets, and has been a reliable method since its first use in 1993 to identify 51 Pegasi b (Mayor & Queloz 1995). Since then, the radial velocity method has produced 21% of all currently confirmed exoplanets. Up until 2013, it was the primary method of detecting exoplanets.

The radial velocity method is related to the mass ratio of the star and the planet. Therefore, this method favors massive planets and low-mass stars, due to the amplifying effect these characteristics have on the overall strength of the RV signal. A new class of exoplanets, dubbed hot Jupiters, describes gas giants that orbit their stars in a matter of days. These planets have a sufficient gravitational pull and distance from their star to cause dramatic spectral line shifts. Low-mass stars overall are more easily influenced by any orbiting bodies they have, provided the planets are massive enough to be detectable by the RV method in the first place. They are also intrinsically faint, and are difficult to achieve precise RV measurements from.

1.2.2 Transits

Photometry reveals planetary parameters that are otherwise undetected by spectroscopic observations. Time-series photometry that detects the passage of the planet in

front of the star, commonly known as the transit method, is responsible for the majority of candidate and confirmed exoplanets. As a planet passes in front of its host star, it blocks a portion of observable light. Photometry taken of a star as this phenomenon occurs can indirectly reveal the presence of orbiting bodies. Transits can reveal a planet's radius and orbital inclination. This method is responsible for the majority of candidate and confirmed exoplanets, and more are still being found within photometry data from the Kepler (Borucki et al. 2010), K2 (Howell et al. 2014), and TESS (Ricker et al. 2015) missions. This method is not without its drawbacks; the system must have an edge-on orbit in relation to the observer to witness the planet pass in front of the star, a feature that is purely coincidental and therefore leaves out the majority of planetary systems. In addition, some stars are too dim to gain sufficient photometry of, regardless of the size and number of their orbiting bodies. While the current number of confirmed exoplanets exceeds 5000, there are probably tens of thousands of systems that have remained undetected due to the biases present within the transit method. Regardless, transit photometry remains a key player in populating our local sky with exoplanet candidates.

These detection methods allow us to see the strengths and weaknesses of what exoplanets exist within this scope of detection. Biases err the resulting population an indeterminate degree away from what could be considered to be a true representation. What we do gain from these findings, however, is responsible for defying expectations on how exoplanets can exist around a multitude of system types. In this next section, I will discuss the implications the host star has on their exoplanets stability and physical parameters, and the limitations of these interactions.

1.3 Stellar Variability and Star-Planet Relationships

All stars, regardless of age, composition, or orbiting bodies, experience some form of stellar variability. This variability can range from periodic stellar flares, to pulsations, star spots, and even asteroseismic oscillations. Any number or combination of these variability types can affect planetary companions with a wide range of results.

Stellar variability can affect both the detection of exoplanets as well as the physical parameters of these exoplanets. Stellar flares directly influence the quality of transit photometry, and can entirely mask or pollute data. Stars with stellar flares could directly affect the thickness and stability of their planet's atmospheres, since the barrage of stellar winds could expose a planet to more damaging radiation than a planet orbiting a non-flaring star (Rodríguez-Mozos & Moya 2019). Star spots can be misinterpreted as orbiting bodies due to the periodic decrease in brightness every stellar rotation. Asteroseismic behavior due to oscillations of the stellar body can interfere with the quality of any spectroscopic data, and therefore render the radial velocity method unusable. While stellar variability can be detected, it is not always correctable, and it remains as a direct effect on any planets within the star's influence.

It needs to be said that while this variability analysis takes into account many stellar parameters, not all of them will be discussed in this study. Some parameters, such as age, cannot be reliably quantified for many stars. Some values, such as metallicity, will not be included due to the lack of results for certain stellar types. For this work, host stars will be distinguished by either being on the main sequence or not on the main sequence to simplify how stellar variability affects certain populations.

In this thesis, I will discuss my research in the context of how stellar variability affects how exoplanets are perceived and how they affect the physical parameters of their exoplanets. In Chapter 2, I will discuss the likely false positive BD-06 1339b and how stellar variability affected how this target was observed. Chapter 3 will then cover the populations of exoplanets with variable stars, as well as how those stars are represented within the overall observable star population.

Chapter 2

Revisiting BD-06 1339b: A Likely False Positive Caused by Stellar Activity [1]

2.1 Introduction

Exoplanets discoveries thus far have been dominated by indirect techniques, mostly due to the success of the radial velocity (RV) and transit techniques. Prior to the discoveries of the Kepler mission (Borucki et al. 2010; Borucki 2016), the majority of exoplanets were discovered using the RV method (Butler et al. 2006; Schneider et al. 2011), with a growing number of ground-based transit discoveries (Konacki et al. 2003; Alonso et al. 2004; Bakos

[1]This chapter contains an article that has been accepted for publication by The Astronomical Journals written by Emilie Simpson, Tara Fetherolf, Stephen R. Kane, Joshua Pepper, Zhexing Li, and Teo Mocnik et al. 2022, arXiv e-prints, arXiv:2203.06191

et al. 2007; Kane et al. 2008). Indirect detection techniques rely on a detailed characterization of the host star, since the properties of the host star determine the extracted planetary parameters (Seager & Mallén-Ornelas 2003; van Belle & von Braun 2009). Of particular importance is the effect of stellar activity, since this can severely limit the detection of exoplanets around active stars (Desort et al. 2007; Aigrain et al. 2012; Zellem et al. 2017), and can even result in false-positive detections, whereby stellar activity cycles can masquerade as exoplanet signatures (Nava et al. 2020). Indeed, there have been numerous instances of exoplanet claims using the RV method that were later determined to be the result of stellar activity (Henry et al. 2002; Robertson & Mahadevan 2014; Robertson et al. 2015; Kane et al. 2016). This potential confusion may be mitigated in certain cases by utilizing precision photometry for known exoplanet hosts (Kane et al. 2009), such as data acquired by transit surveys. A transit detection of an RV planet can provide confirmation of the planet, as well as provide an additional means to disentangle stellar variability and planetary signatures (Boisse et al. 2011; Díaz et al. 2018). The Transiting Exoplanet Survey Satellite (TESS) (Ricker et al. 2015) provides an invaluable photometric data source for known exoplanet hosts (Kane et al. 2021) since it is monitoring most of the sky, and is especially well-suited for observing the bright host stars typical of RV exoplanet searches (Fischer et al. 2016).

Stellar activity has long been known to affect and sometimes limit RV exoplanet searches (Saar & Donahue 1997), and can particularly impact detection of planets within the Habitable Zone (Vanderburg et al. 2016). Photometric monitoring of known host stars has been used in numerous cases to determine the effects of their variability on planetary

signatures, such as for HD 63454 (Kane et al. 2011) and HD 192263 (Dragomir et al. 2012). Another example of a host star exhibiting significant stellar variability is the case of BD-06 1339, which was discovered to host planets by Lo Curto et al. (2013) using data from the High Accuracy Radial velocity Planet Searcher (HARPS) spectrograph (Pepe et al. 2000). These observations revealed two planetary signatures with orbital periods of 3.87 days and 125.94 days, with minimum planetary masses of 0.027 and 0.17 M_J, respectively. However, photometry of sufficient precision, cadence, and duration was not available in order to confirm a transit signature.

Here, we present an investigation into the BD-06 1339b planetary signature by analyzing the associated TESS photometry and re-analyzing the existing HARPS RV data. In Section 2.2, we discuss the properties of the system, including the stellar parameters, and the possible planets within the system. Section 2.3 describes the data analysis for the system, where the data sources are comprised of HARPS RV data and the precision photometry from TESS. Section 2.4 combines these results to present an argument that the RV variations originally detected could alternatively be consistent with the intrinsic variability of the host star. We provide concluding remarks in Section 2.5, and outline how the photometric capabilities from TESS not only serve to discover new planets, but also have considerable utility in testing known exoplanet hypotheses

2.2 System Properties

BD-06 1339 (HIP 27803, GJ 221, TIC 66914642) is a relatively bright high proper-motion star located at a distance of 20.27 pcs (Gaia Collaboration et al. 2018, 2021). Ac-

cording to Lo Curto et al. (2013), BD-06 1339 is a late-type dwarf star, with a spectral classification of K7V/M0V and an age similar to that of the Sun. The star has an effective temperature of 4324 K, a V magnitude of 9.70, and a stellar mass of 0.7 $M_{\odot}$. Initial spectroscopic analyses were performed in 1996 for the Palomar/MSU Nearby Star Spectroscopic Survey (Hawley et al. 1996) among previously reported variable stars. A further survey of chromospheric activity among cool stars by Boro Saikia et al. (2018) found that BD-06 1339 is moderately active, with an activity index of $\log R'_{HK} = -4.71$. Such magnetic activity is prevalent in later stellar spectral types (McQuillan et al. 2012), lending to the stellar activity of interest for this study.

The host star is currently reported to have two companions, BD-06 1339b and BD-06 1339c, both of planetary mass and discovered via the RV technique (Lo Curto et al. 2013). Though discovered simultaneously, their properties differ greatly; BD-06 1339b has a minimum mass of 8.5 $M_{\oplus}$ and orbits its host star in 3.873 days at a semi-major axis of 0.0428 AU. Its sibling, BD-06 1339c, has a minimum mass of 53 $M_{\oplus}$, has an orbital period 125.94 days at a semi-major axis of 0.435 AU. The Lo Curto et al. (2013) analysis of the RV data for BD-06 1339b adopts a fixed circular orbit ($e = 0$) for the b planet, and derives an eccentricity of 0.31 for the c planet. Tuomi (2014) conducted a statistical reanalysis of the RVs for BD-06 1339, which we further investigate in Section 2.3.1.

2.3 Data Analysis

The motivation for re-analyzing BD-06 1339b stems from a broad stellar variability analysis of stars observed during the TESS primary mission at 2-min cadence (Fetherolf

et al. in prep.), and a further investigation into the stellar variability of known exoplanet host stars (Simpson et al. in prep.). The broad stellar variability analysis by Fetherolf et al. (in prep.) searches for periodic photometric modulations on timescales up to the duration of a single orbit of the TESS spacecraft (0.01–13 days), during which TESS obtained continuous observations. The ∼700 exoplanet host stars that were selected for the follow-up variability analysis by Simpson et al. (in prep.) includes planets with orbital periods shorter than 13 days that were discovered by either their RV or transit signatures. Since Kepler exoplanet host stars are typically faint and not ideal for RV follow-up observations, they are not included in the stellar variability analysis of known exoplanet host stars. In addition to possible transit events or variations due to stellar activity, some of these planets may also exhibit interactions with their host stars, such as phase variations or star-surface irregularities.

The full TESS light curve, Lomb-Scargle (L-S) periodogram, and light curve that was phase-folded on the most significant photometric variability signature were each visually inspected for the ∼700 known exoplanet host stars. The photometric periodicity was determined to be significantly variable if both the normalized and phase-folded light curves displayed sinusoidal behavior that did not align with known spacecraft systematics (i.e., momentum dumps), and if the periodogram maximum exhibited an isolated peak with at least 0.001 normalized power that also exceeded the 0.01 false alarm probability level. For each known exoplanet, the extracted photometric variability period was compared to their orbital period, as reported by either the TESS Objects of Interest (TOI) catalog (Guerrero et al. 2021) or by cross-referencing the target in the NASA Exoplanet Archive (NASA Ex-

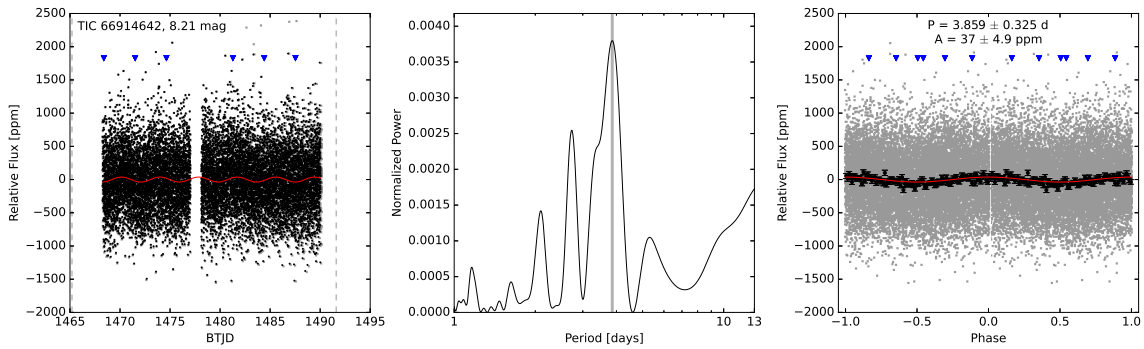

Figure 2.1 The TESS light curve (left), periodogram (center), and phase-folded light curve (right) of BD-06 1339. The red curve represents a sinusoidal model fit representing the light curve variability. The blue triangles indicate timings of spacecraft thruster firings (i.e., momentum dumps). This system stood out in our visual analysis because of its pronounced sinusoidal behavior and the strong single peak in the periodogram, which indicates a strong variability signal. The detected variability periodicity (3.859 days) is only 0.03% away from the reported orbital period for BD-06 1339b (3.873 days).

oplanet Archive 2021). Close-period matches between the photometric variability and the planetary orbital period were defined as being within 5–10% of each other. Out of the ∼700 targets subjected to the visual analysis, approximately 180 systems displayed prominent photometric variable behavior, close-period matches, or both.

BD-06 1339b was among the set of targets that matched these criteria, and the resulting TESS light curve, periodogram, and phase-folded light curve are shown in Figure 2.1 (see also Section 2.3.2). In this paper we revisit the analysis of the BD-06 1339 system by including the TESS photometry that was unavailable at the time of previous studies. In Section 2.3.1 we summarize our re-analysis of the RVs using the data provided by the updated HARPS reduction pipeline (Trifonov et al. 2020). We then discuss our in-depth analysis of the TESS photometry in Section 2.3.2, where we search for the presence of planetary transits, atmospheric variations, and stellar activity.

2.3.1 Spectroscopic Analysis

Lo Curto et al. (2013) verified the planets orbiting BD-06 1339 by requiring the normalized fourier power of the L-S periodogram of the RV time series to have a false alarm probability of $< 10^{-4}$. The $\log R'_{HK}$ activity index was considered poor quality, and therefore was not utilized in the overall analysis. BD-06 1339b was barely discernible within the RV signal of BD-06 1339c in this stage of analysis, existing initially as additional variations. To verify the planetary nature of this signal, the founding team cut the datasets in half to exclude long-term trends. These variations then increased in strength throughout the observation period as the Ca II H re-emission decreased. The discovery team was unable to determine any other longer-term trends due to their limited window of 102 observations over 8 years. They determined that BD-06 1339 b was an educational case of how planets can hide within the activity of variable stars.

To further analyze the BD-06 1339 system, (Tuomi 2014) implemented a more meticulous probability check involving an independent statistical method of subsequent samplings and the utilization of log-Bayesian evidence ratios. The Bayesian analysis used by Tuomi (2014) evaluated the RV time series as if they were observed in real time. At each iteration, a "new" RV measurement was added to the dataset from which the best-fit system parameters were determined. In this case, they utilized HARPS and Planet Finder Spectrograph (PFS; Crane et al. 2010) velocities in their credibility tests. HARPS found the planetary signals of the two original targets and consistent with each other. PFS could not discern any signals previously found by Lo Curto et al. (2013). The system itself was not explicitly observed for this publication, instead relying on the previous data available

at the time. Their results focused on the discovery of a third d planet at a ∼400 day orbital period based on a statistical probability, and they considered BD-06 1339b as a confirmed planet.

The observations of BD-06 1339 were acquired by the HARPS team and originally published by (Lo Curto et al. 2013). The data has since been re-reduced and includes corrections of several systematics within the observations (Trifonov et al. 2020). With the improved precision and availability of the data, a re-analysis could derive the orbital parameters of the known companions in the system with better precision and potentially reveal smaller signals that were previously unreported before the re-reduction of the RVs.

We performed a re-analysis of the RVs for BD-06 1339 using the re-reduced data published by Trifonov et al. (2020). We first ran an RV Keplerian periodogram on the dataset to search for significant signals using `RVSearch` (Rosenthal et al. 2021). The `RVSearch` algorithm iteratively searches for periodic signals present in the dataset and calculates the change in the Bayesian Information Criterion (ΔBIC) between the model at the current grid and the best fit model based on the goodness of the fit. The result of the search would yield signals that are of planetary origin as well as those that are due to stellar activity. We adopted signals returned by `RVSearch` if they peak above the 0.1% false alarm probability level. The search returned two significant signals, one at 125 days and another at 3.9 days. This is consistent with the results from Lo Curto et al. (2013).

We then used the RV modeling toolkit `RadVel` (Fulton et al. 2018) to fully explore the orbital parameters of these two signals and to assess their associated uncertainties. We provided the orbital parameter initial guesses for the two signals using the values returned

by `RVSearch` and allowed all parameters to vary, including an RV vertical offset, RV jitter, and a linear trend. We fit the data with maximum a posteriori estimation and explored the posteriors of the parameters though Markov Chain Monte Carlo (MCMC). The MCMC exploration successfully converged and we show the results in below.

Orbital parameters of the two signals are mostly consistent with those reported by Lo Curto et al. (2013), except that the orbit of the c planet is preferred to be nearly circular ($e_c \sim 0.09$) instead of a mildly eccentric ($e \sim 0.31$), as proposed by (Lo Curto et al. 2013). In addition, there appears to be a significant linear trend ($\sim 7\sigma$) present in the data that could be indicative of an additional long orbital period massive companion orbiting in the outer regime of this system. Both the linear trend and two circular orbits model are supported by Bayesian model comparisons. The RV signature for BD-06 1339b is shown in left panel of where the contribution from the c planet has been removed. The results of this latest RV re-analysis are consistent within the uncertainties of the original analysis performed by Lo Curto et al. (2013).

2.3.2 Photometric Analysis

Gillon et al. (2017) used the Warm mode of the Spitzer mission to search for transits of 24 low-mass planets (all single planet systems) discovered through the RV method, including BD-06 1339b. The Spitzer photometry found no reliable transits for 19 of the 24 planets, including BD-06 1339b. Specifically, BD-06 1339b was found to not display a transit within the observation window, although the photometry did not cover approximately 20% of the possible transit window. Since then, TESS observed BD-06 1339 at 2-min ca-

Table 2.1. Updated RV System Parameters of BD-06 1339.

Parameters	b	c
P (days)	$3.87302^{+0.00036}_{-0.00033}$	125.49 ± 0.13
Tc (BJD)	$2455000.91^{+0.21}_{-0.17}$	$2455279.6^{+2.0}_{-1.8}$
Tp (BJD)	$2455001.65^{+0.39}_{-0.62}$	2455285^{+16}_{-14}
e	$0.22^{+0.16}_{-0.13}$	$0.089^{+0.054}_{-0.052}$
ω (deg)	$181.23^{+38.39}_{-55.00}$	$110.58^{+49.27}_{-38.39}$
K (m s^{-1})	$3.47^{+0.52}_{-0.49}$	$8.32^{+0.46}_{-0.47}$
M_p ($M_{\rm E}$)	$6.45^{+1.0}_{-0.98}$	$50.9^{+4.5}_{-4.4}$
a (au)	$0.0429^{+0.0014}_{-0.0015}$	$0.436^{+0.014}_{-0.015}$

Note. — ω values are those of the star, not of the planet. The RV fit includes a linear trend of $\dot{\gamma} = -0.00239^{+0.00032}_{-0.00033}$ m s^{-1} d^{-1}.

dence nearly continuously during the observations of Sector 6. In this section, we use to the TESS photometry to search for transits by either the b or c planets and atmospheric phase variations caused by the b planet.

BD-06 1339 was observed during TESS Sector 6 (2018 Dec 11–2019 Jan 07) at 2-min cadence and TESS Sector 33 (2020 Dec 17–2021 Jan 13) at 30-min cadence. The TESS light curves and full-frame images are publicly available through the Mikulski Archive for Space Telescopes[2] (MAST). Since the anticipated transit of BD-06 1339b is on the order of $\sim$2 hr, we elect to only use the 2-min cadence light curve from the Sector 6 observations. We use the original data release of the pre-search data conditioning (PDC) light curve that was processed by the Science Processing Operations Center (SPOC) pipeline (Jenkins et al.

[2] https://archive.stsci.edu/

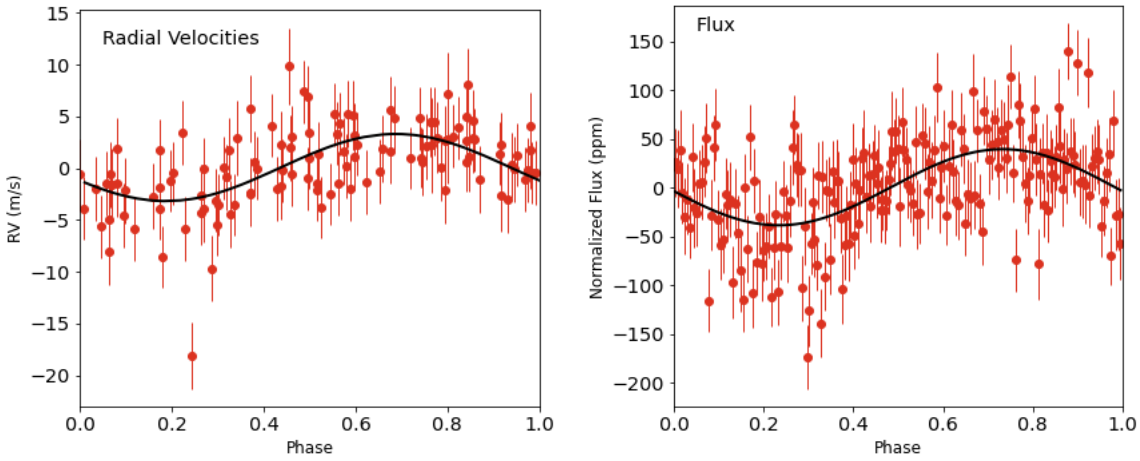

Figure 2.2 Left: The RV signature of BD-06 1339b (c planet's signal removed). Right: The TESS photometry phase-folded on the orbit of BD-06 1339b. The black curves represent sinusoidal fits to the data.

2016) and additionally remove any observations denoted with poor quality flags or that are 5σ outliers. The L-S periodogram (Lomb 1976; Scargle 1982) is then computed on the BD-06 1339 light curve using an even frequency spacing of $1.35\,\mathrm{min}^{-1}$, where we find a maximum normalized power of $\sim$0.0038 at 3.859 ± 0.325 days. The 0.01 false alarm probability level for the periodogram of the BD-06 1339 light curve corresponds to 0.0012 normalized power, with the peak of the periodogram having a $\ll 10^{-4}$ false alarm probability.

Our L-S periodogram analysis of the TESS light curve reveals a sinusoidal periodicity that is consistent with the orbital period of the b planet (3.8728 ± 0.0004 days) within their uncertainties (see Figure 2.1). A planet's orbital period may be extracted from a periodogram analysis if transit events are not properly removed from the observed light curve. However, we do not observe transit events by either the b or c planets in the TESS photometry , which is consistent with the findings of (Gillon et al. 2017). A significant sinusoidal amplitude could also indicate the presence of a planet-induced photometric phase curve

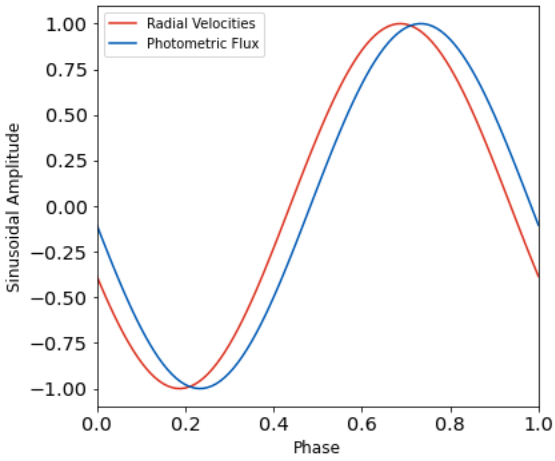

Figure 2.3 The sinusoidal fits to the RV (red) and flux (blue) curves from Figure 2.2, but with the amplitudes normalized to unity. A strong correlation in the phase offset can be seen around 0.7 phase.

caused by its day-side reflection or excess thermal emission. If the phase curve is caused by the day-side reflection of the planet, then the maximum brightness of the phase-folded light curve is expected to peak at 0.5 phase when we see the greatest area of the planet illuminated from our point of view. Alternatively, atmospheric winds that redistribute heat from the day to night-side could cause the hottest region of the atmosphere to be shifted eastwards from the sub-stellar point, such that the phase-folded light curve peaks prior to 0.5 phase (e.g., Showman et al. 2013; Heng & Showman 2015).

We use the measured time of conjunction (i.e., expected transit time) from the RV analysis to assess both the shape and phase of maximum amplitude of the TESS phase-folded light curve for BD-06 1339b. The full phase curve is fit using a double harmonic sinusoidal function, which allows for modulations caused by Doppler boosting and ellipsoidal variations in addition to the reflection caused by the day-side of the planet (see Shporer 2017). The first cosine harmonic component represents the modulations caused by day-side reflection or

thermal emission, such that the maximum brightness occurs at 0.5 phase. The phase-folded light curve of BD-06 1339b exhibits a significant sinusoidal modulation of ∼40 ppm in the TESS photometry (see right panel of with a maximum brightness at the third quadrature of the b planet's orbital phase (0.73 phase). In addition to the maximum brightness being at a phase that is inconsistent with day-side reflection or thermal emission, the amplitude of the phase curve is ∼10 times greater than expected for such a small planet.[3]

2.4 False-Positive Planetary Signature?

The results described above cast doubt on the planetary origin of the signal ascribed to BD-06 1339b. This target may, in fact, instead be a possible case for the stellar variability of the host star masquerading as a false positive. While it is not impossible for a system to exist in which a planet orbits at the same period as its host star's variability, a coincidence of 0.01 days between the two is highly unlikely. A visual comparison of the RVs and stellar flux of the host star is enough to raise some questions, but we must quantify our results. We further investigate the nature of BD-06 1339b by comparing the phase signature in the RVs and photometry, searching for correlations in the spectral activity indicators, and considering the likelihood of BD-06 1339 exhibiting periodic stellar activity at ∼3.9 days.

Figure 2.2 shows the RV signature and the photometric variations in phase with the anticipated orbit of BD-06 1339b. We fit a simple sinusoidal function to each phase

[3]The day-side reflection modulations of 8.5 $M_\oplus$ planet with an albedo of 0.3 are expected to be on the order of ∼2 ppm.

curve and find that the maximum of the RVs occurs at 0.69 phase with an amplitude[4] of $3.3\,\mathrm{m\,s^{-1}}$, and the maximum of the photometric flux occurs at 0.73 phase with an amplitude of 40 ppm. Interestingly, the RVs and the photometric variations peak at approximately the same phase. The correlation between these sinusoidal functions is further emphasized in Figure 2.3, where the two functions are normalized by having their amplitudes set to unity.

Clearly there is a very strong correlation between the RVs and the photometry, but they should instead be offset from each other in phase. If the photometric variations were caused by atmospheric reflection or thermal emission of BD-06 1339b, the photometric variations should peak at 0.5 phase or earlier due to winds (e.g., Showman et al. 2013; Heng & Showman 2015). However, the observed phase offset is subject to uncertainties from the time of conjunction determined from the RVs (0.2 days) and the time between the RV and TESS observations (∼3500 days). Propagating the time of conjunction, and thus phase offset, out to the time of the TESS observations results in an uncertainty of 0.5 days (13% of the orbital period), which could render the correlation in phase between the RVs and photometry as a coincidence.

In addition to the photometry, we performed an analysis on all of the available RV activity spectral indicators provided by the HARPS RV database (Trifonov et al. 2020) to investigate whether any significant activity signals are consistent with the reported period for BD-06 1339b. We used a Generalized L-S periodogram (GLS; Zechmeister & Kürster 2009) to search for periodicity in H_α, chromatic index (CRX), differential line width (dLW) (Zechmeister et al. 2018), as well as full-width-at-half-maximum (FWHM) and contrast of the cross correlation function (CCF). None of the aforementioned indicators returned

[4]This amplitude is estimated assuming a simple sinusoidal function, and thus a zero eccentricity.

significant signals above the 0.1% false alarm probability level, except for dLW where a $\sim$ 270-day signal was detected just above the false alarm probability threshold and is possibly of stellar activity origin.

We also investigated if there exists any correlation between the b planet's RV signal (after the removal of RV contributions from the c planet and the linear trend) and each one of the activity indicators using the Pearson correlation coefficient. Once again, only dLW returns a weak correlation of ~ 0.25, while there is no correlation observed in any of the other activity indicators. While there is no peak in the dLW periodogram near $\sim$ 3–4 days, the correlation between the b planet's RV signature and dLW could be related to the 270-day signal. Overall, despite the strong indication from the photometry that the previously reported b signal could attributed to stellar activity, no significant correlations were found between the b planet's RVs and any of the spectral activity indicators, and no activity periods were detected near the b planet's orbital period.

This raises the question of how stellar variability can be selectively manifesting in the photometry, but not in the spectral lines of the host star. We investigate whether the signal observed in the BD-06 1339 light curve is typical for stars of similar spectral types. From the all-sky variability analysis, we searched for stars with effective temperatures between 4000–4500 K, photometric variability periods of 3.5–4.0 days, and stellar luminosities lower than $10\,L_{\odot}$. We find $\sim$30 stars within this subgroup and, upon visual investigation, find that their light curves are similar in shape and amplitude to the variations observed for BD-06 1339 (see Figure 2.1). Their light curve behavior proved to be comparable to

what is observed in the BD-06 1339 light curve. Therefore, stellar activity is a potential explanation for the observed photometric variations.

We cannot pinpoint the physical mechanism behind the photometric variability, although our general understanding of stellar astrophysics suggests that it is related to magnetic activity in the star that produces spots and plages. The false alarm probability (Lo Curto et al. 2013) used to detect BD-06 1339b was based on a simple f-test, but recent work has shown that other statistical methods, such as the extreme value statistical distribution, may be more appropriate for applying to periodogram analyses (Süveges 2014; Vio & Andreani 2016; Sulis et al. 2017; Vio et al. 2019; Delisle et al. 2020). The close match between both the period and phase of the photometric variability and the RV variations suggests that both signals are produced by the same cause. We therefore believe that the most likely explanation is that BD-06 1339b is a false positive and that the RV variations are not produced by a planetary companion of the star.

2.5 Conclusions

We conducted a photometric analysis of targets with periodic modulations from the TESS primary mission (Fetherolf et al. in prep.; Simpson et al. in prep.) and determined that BD-06 1339b was considered a prime subject for further scrutiny. The similarity between the photometric variability periodicity of the TESS photometry for BD-06 1339 (3.859 days) and the orbital period of the b planet (3.874 days) prompted a rigorous re-examination of the spectroscopy and photometry for this target. We performed a re-analysis of the RVs obtained by HARPS and found an orbital solution that was consistent with the

RV analysis performed by Lo Curto et al. (2013). An in-depth investigation of the photometric variations revealed that they were inconsistent with atmospheric phase variations due to the planet based on their phase and amplitude, but they could possibly be attributed to stellar activity. Comparing the RV analysis with the phase-folded photometric fluxes (see Figure 2.2)) revealed a strong correlation between the two datasets (see Figure 2.3).

With these results in mind, we addressed what this means for the interpretation of the RV modulation observed near 3.9 days, previously attributed to a planetary signal. Stellar activity is a possible culprit, but the spectroscopic emission lines of this star do not correlate well with the photometric modulations of this star. Therefore, there is a wide field of opportunity for this target to be analyzed further to determine the source of the discrepancy between the photometric and spectroscopic behavior.

These results indicate that BD-06 1339b is, in fact, a likely false positive whose signature was induced by the activity of the star. Follow-up observations could help to resolve the discrepancy between the photometric and spectroscopic data. In particular, understanding the nature of the discrepancy would benefit from additional precision photometry of the star to improve the characterization of the stellar variability, alongside simultaneous spectroscopic activity indicators (Díaz et al. 2018) and an extended RV baseline. Overall, reanalysis of this systems emphasizes the greater importance of further verifying the nature of confirmed RV planets as new data becomes available—especially for those that are low in mass and of high interest to demographics and atmospheric studies.

Chapter 3

Stellar Variability of Known Hosts Observed by TESS[1]

3.1 Introduction

Over the course of exoplanetary science, the methods used to detect planetary bodies have changed and evolved. With the successful launch and calibration of the James Webb Space Telescope (Gardner et al. 2006) and the prolific findings of former and current missions such as Kepler (Borucki et al. 2010), K2 (Howell et al. 2014), and TESS (Ricker et al. 2015), the catalog of candidate and confirmed exoplanets continues to grow.

Part of the exoplanet identification process relies on the characteristics of the host star. Parameters such as age, composition, size, and temperature can affect the formation and stability of a planetary system, as well as the resulting features of those planets. At-

[1]This chapter contains a draft of an article being prepared for submission to The Astronomical Journals, written by Emilie Simpson, Tara Fetherolf, Stephen Kane, Joshua Pepper, and Teo Mocnik, with an expected submission of June 2022.

mosphere formation and composition is a prevalent example: it can determine whether the exoplanet can host and sustain life (Ribas et al. 2005), as well as answer questions regarding our own Earth's journey to habitability (Kopparapu et al. 2014; Lammer et al. 2007; Segura et al. 2010).

This study will focus on how the photometric modulations of the host star are represented in different stellar types and how it affects their exoplanets. We begin with a broad variability analysis of stars observed at 2-minute cadence from the primary mission of TESS, then narrow down the population to a select amount of sufficiently variable targets. Known hosts within this group of variable stars are then subjected to cross-correlation in search of any defining features of either the host star or their planetary companions. We then discuss the implications of these results on confirmed and candidate exoplanets, as well as how these findings can be applied to future exoplanet discoveries.

3.2 Data Analysis

Targets were observed at 2-minute cadence during the primary mission of TESS (Cycles 1 and 2). The full population of stars comes from an all-sky broad variability analysis conducted by Fetherolf et al. (in prep) in search of short-period variability on a 0.01–13 day timescale. This timescale was chosen to reflect the orbit duration of the TESS spacecraft, and therefore to emphasize targets with continuous observations and to minimize spacecraft systematics. Approximately 230,000 stars worth of TESS photometric data and stellar properties extracted from the TICv8 catalog (Stassun et al. 2019) were analyzed.

A series of cutoffs were required to ensure that the stars included in this test population had strong enough variability to both be sufficiently detectable and to directly affect their planets. The first of these cutoffs ensured that stars were sufficiently bright (greater than 14 magnitude) and had less than 20% contamination from neighboring stars. Another cutoff required normalized power to be greater than 0.001 so that the variability signal would be strong enough to show within the TESS photometry. Targets that were contaminated with spacecraft systematics such as periodic pointing corrections (i.e. momentum dumps) were also cut entirely.

This left approximately 50,000 stars as sources of stellar variability. From this population, 644 stars were known to be exoplanet hosts. Now that we had targets that were sufficiently variable regardless of the source, targets now needed to be assessed based on the periodic nature of the associated variability. For this work, we focused on stars that exhibited periodic short-period variability (¡13 days). This required a comprehensive Lomb-Scargle periodogram analysis (Lomb 1976; Scargle 1982) and inspection of the phase-folded lightcurve.

Figure 3.1 represents the target HAT-P-34b and is a prime example of what is considered to be sufficient and desired stellar variability for these targets. We consider one- and two-peak solutions above 0.1 normalized power that are well-isolated from other signals in the periodogram. A sinusoidal fit to the lightcurve as well as the phase-folded lightcurve ensures that the variability is periodic in nature as opposed to being a result of single-event occurrences. Blue markers indicating the location of momentum dumps were added as a precaution to identify possible spacecraft systematic interference in the event it

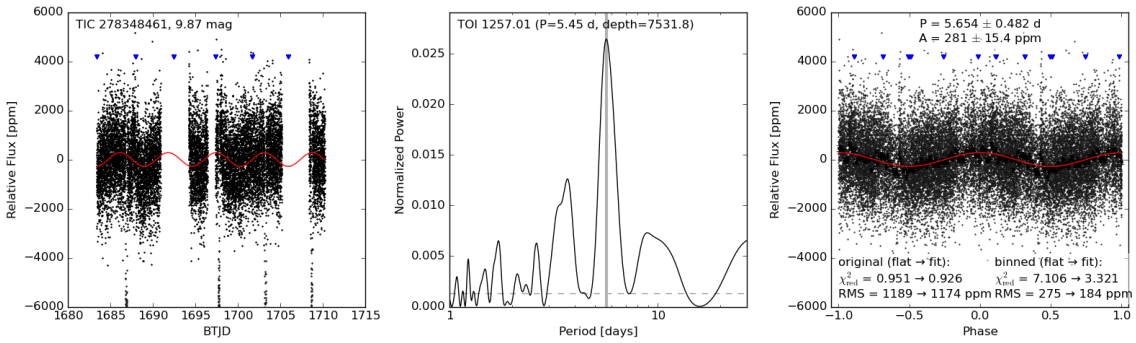

Figure 3.1 An example Lomb-Scargle periodogram analysis of the target HAT-P-34. Left: the normalized lightcurve of HAT-P-34 with a red sinusoidal fit line and momentum dump flags. Center: the LS periodogram, and the associated TOI information. Right: the phase-folded lightcurve of HAT-P-34, with blue momentum-dump flags and a red sinusoidal fit line.

is masquerading as a stellar variability signal. A "real" variability signature would result in an even dispersal of these blue markers across both the lightcurve and the phase-folded lightcurve, while a signal caused by momentum dumps would have the flags appear grouped on peaks and troughs of the sinusoidal shape of the phase-folded lightcurve. After this visual analysis, 427 targets remained for the overall variable known hosts analysis. In these next sections, we will discuss how these targets are represented among the initial all-sky variable star population as well as the population of confirmed exoplanet hosts.

3.3 Population Analysis

Now that we have the final population of targets for the variability analysis, we can compare their parameters against each other to see whether any correlations exist between the two. While many parameters could lend themselves to this analysis, we will focus on stellar parameters that can directly affect planetary characteristics such as effective temperature, radius, variability period, and power amplitude. For clarification, the stellar

Table 3.1. Known Hosts Table

TIC ID	Planet Name	$P_{\rm orb}$ (days)	$P_{\rm var}$ (days)
TIC 100100827	WASP-18 b	0.94145223	0.470567
–	WASP-18 c	2.1558	–
TIC 101721385	HAT-P-14 b	4.62767	1.000917
TIC 101955023	GJ 1132 b	1.628931	7.256636
–	GJ 1132 c	8.929	–
TIC 102987456	HD 24064 b	535.59998	3.695204
TIC 103633434	TOI-1235 b	3.444717	1.000118
TIC 105438311	HD 81688 b	184.02	1.286181
TIC 106760549	HD 92987 b	10354.8375	0.257287
TIC 111947706	HIP 67851 b	88.9	0.42677
–	HIP 67851 c	2131.8	–
TIC 1129033	WASP-77 A b	1.36002854	5.544999
TIC 114807081	HD 224693 b	26.6904	10.027146

Note. — Listed are the first ten objects in our catalog. The complete table will be available electronically in the published manuscript.

parameters are being sourced from the TICv8 catalog, while the planetary parameters are being sourced from the NASA Exoplanet Archive. Luminosity values are calculated with TICv8 radius and effective temperature values; reported luminosity values are not used here.

Figure 3.2 shows two plots the one on the left displaying the initial all-sky variable star population and the one on the right displaying the final variable known hosts population. Between the two plots, there are shifts in both population density and variability dispersion. In the all-sky variability analysis, there is a high concentration of high-amplitude

targets in the main sequence. This differs from the final variable known hosts population, which has low-variability targets make up the main sequence and higher-amplitude values in the low-mass and giant branches. This can be traced to the solution types present in both of these populations.

There are three main identifiers for these variable targets: 1-peak, 2-peak, and auto-correlative function (ACF) targets. In the initial all-sky population, all the high-amplitude targets in the main sequence were either ACF or 2-peak solutions. The final population has a 1-peak majority, eliminating almost all of the high-amplitude targets within the main sequence. The loss of these targets can be attributed to the filtering process and the bias towards strong periodic behavior.

There is also a gap where the K-dwarf stars should be. While K-dwarfs are overall abundant in the observable sky, they are not prominent in TESS photometry and therefore are not well-represented. K-dwarf stars are also not very variable, making their absence a result of the initial search for strong variability.

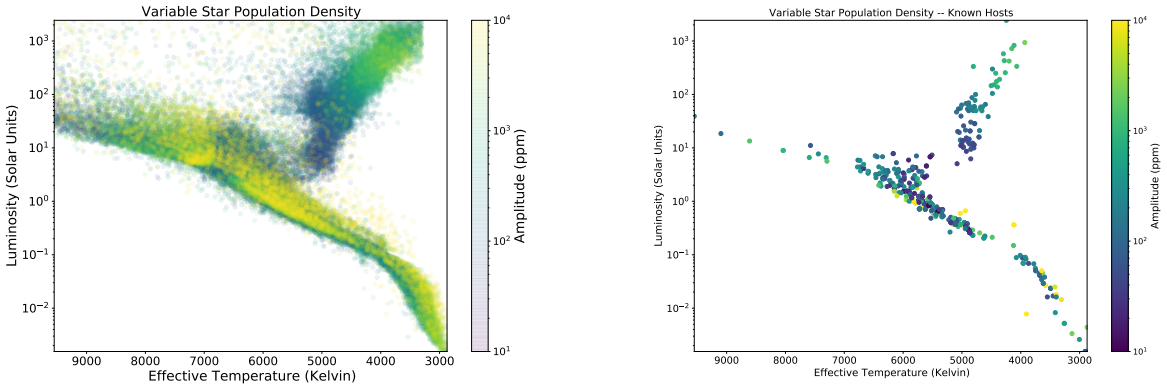

Figure 3.2 Left: The initial population of variable stars colored by amplitude in parts per million (ppm). Right: The final population of variable known exoplanet hosts. Note that both have differing amplitude patterns.

This section will be split into two separate analyses: the final population of exoplanets of these variable stars, and the population of variable stars themselves. These two population studies can reveal a more complete profile of these variable stars and how they affect their exoplanets.

3.3.1 Planetary

This study has revealed 427 planets that call variable stars their home. The hosts' stellar activity is the only shared trait among these targets; any other correlations are indicative of the effect these variable stars have on their planets. Figures 3.3 and 3.4 contextualize where these planets lie among the overall population of confirmed exoplanets. Figure 3.3 shows their locations on a mass-radius diagram, where Figure 3.4 compares radius and orbital period.

There are some features of both the mass-radius plot and the radius vs. orbital period plot that discern these exoplanets from the entirety of the known host population. A slight gap can be discerned at the location of the Fulton gap (Fulton et al. 2017), but it is not very discernible.

In addition, there are more higher-amplitude host stars with higher-radius exoplanets. This is expected due to larger planets being more easily discerned from stars with strong variability. The transit photometry of larger planets against variable stars is easily discerned compared to a smaller target who's transits could be masked by the activity of the star.

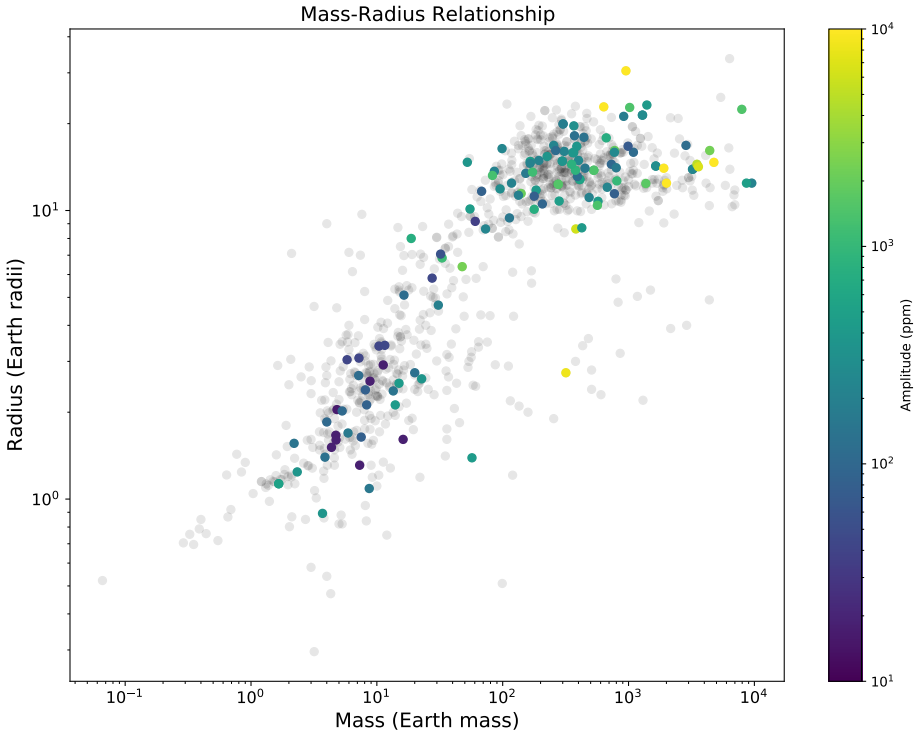

Figure 3.3 A scatter plot that represents the mass-radius relationship of known planets around variable stars. Points in grey represent the overall population of confirmed exoplanets as of 20 May 2022

These planets are well-distributed against the population of confirmed exoplanets. Cutoffs that exist within the data can be attributed to detection biases; it is of no surprise that a prominent group of high-radius exoplanets dominates our sample of planets around variable stars as they are the easiest to detect against even highly variable stars. Some targets have more confirmed parameters than others, making some comparisons impossible. We will now move to the identities of their host stars in hope of revealing any correlations.

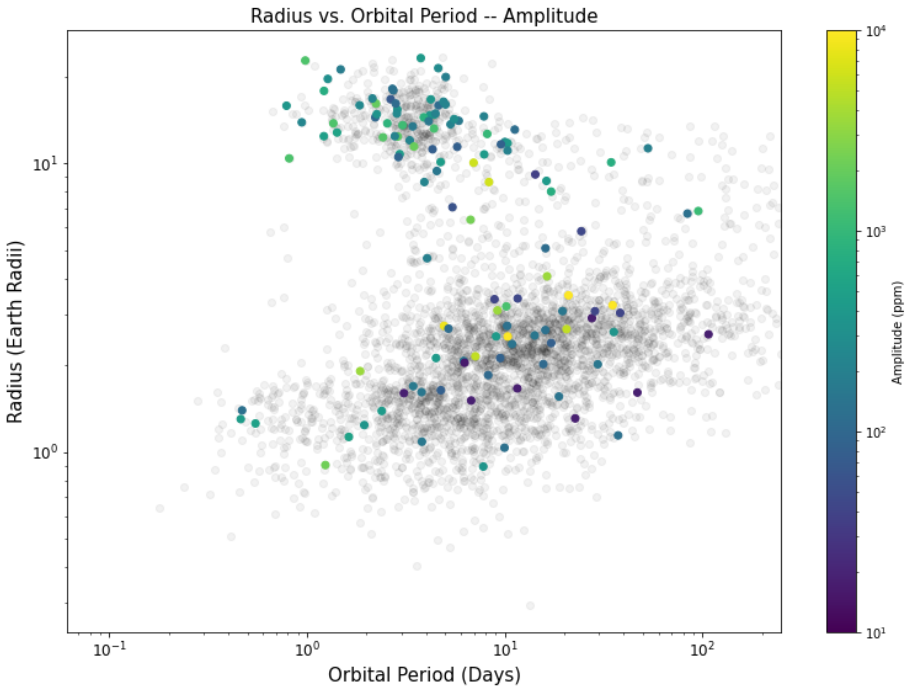

Figure 3.4 A scatter plot of the exoplanets of the variable host stars colored by photometric variability amplitude in ppm. The points in grey are all confirmed exoplanets as of 20 May 2022.

3.3.2 Stellar

Know thy planet, know thy star. While the analysis of the variable host star's exoplanets was useful, the more extensive photometric and spectroscopic data we have on the hosts themselves has the potential to reveal more about the star-planet relationship. We begin by plotting these targets with respect to the primary detection method of their planets.

Figure 3.5 displays the detection method utilized to confirm their planets. We can see here how observational biases favor certain stellar types: planets around giant stars

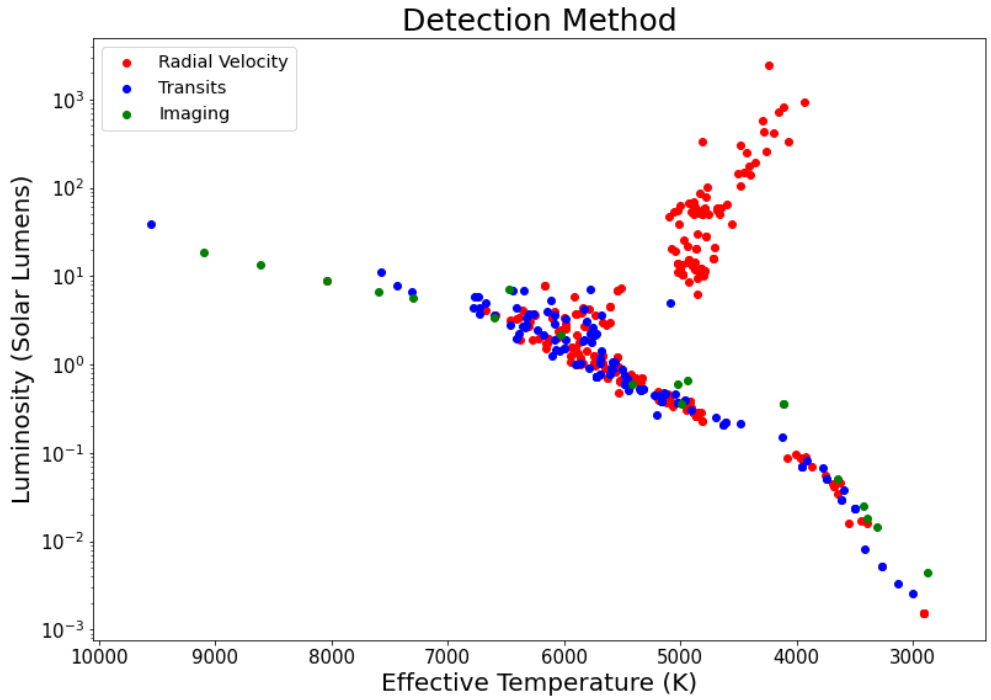

Figure 3.5 The variable stars with known exoplanets known hosts colored by the detection method of their planets.

are more likely to be found via their gravitational influence (i.e., radial velocity method) rather than transit photometry. Dim, small stars are especially subject to influence from gravitational pull from their planets. Transit photometry is also effective for these stars due to the radius ratio; small planets are more easily found around small stars.

There are some outliers within this plot that are unusual for what one expects these detection methods to favor. These targets may lend themselves to a more diverse understanding of the star-planet connections that exist in this population.

KELT-9

KELT-9 can be found at the tail of the blue giants. Its only planet, KELT-9b, was found by a team specializing in exoplanets of "retiring" A-type stars (stars evolving off the main sequence) (Gaudi et al. 2017). This target was initially found via the transit photometry, but was then confirmed with the radial velocity method by the founding team. As these giant stars cool down, they decrease in variability, and interfere less with Doppler spectroscopy. The exoplanet itself is considered an ultra-hot Jupiter. Not only was this planet found orbiting a star that is otherwise far too active and luminous to allow good transit photometry, but this planet also orbits very close to its star at 0.03462 ± 0.0001 AU with an orbital period of 1.48 days. This target is a great example of how decreases in stellar variability can allow for the detection of exoplanets otherwise impossible to detect.

GJ 1061 and GJ 3512

These two host stars are very close to each other, and make up the tip of the low-mass star branch as two radial velocity solutions. While the radial velocity method is a viable method for low-mass stars, these targets could also have interesting implications on how variable low-mass stars affect their planets.

GJ 1061 (Dreizler et al. 2020) is a system of three planets that were all detected via the RedDots campaigns, specializing in exoplanets orbiting low-mass stars. GJ 1061 was observed for three months with the HARPS spectrograph (Mayor et al. 2003). The founding team confirmed three planets orbiting the star, with a fourth signal that could be due to either stellar activity or a fourth planet. The reported fourth signal from this system

is estimated at either 53 or 130 days. We cannot compare the variability results we see from our data with the reported signal, as this study was limited to short-period variability capped at 13 days.

GJ 3512 hosts a single planet, found by (Morales et al. 2019) after an extensive RV analysis. This star is prevalent in magnetic activity, but according to their analysis it does not affect the planet in any way. This target is unique in the 203-day orbit and its eccentricity of 0.4396 ± 0.0042 is very high compared to similar targets. This eccentricity is attributed to planet-planet interactions, with the other planet having been ejected some time before GJ 3512b's discovery. GJ 3512 has a unique insight into how planets of low-mass stars are affected by ejected companions. Whether the variability of the host star affected the ejection of the former planet remains to be seen.

HD 221416

This star lies as a transit solution just underneath the giant branch. HD 221416b was found via TESS transit photometry (Huber et al. 2019) and is the first of its kind to be found orbiting a star exhibiting asteroseismic pulsations. These oscillations are known to be revolutionary in determining the interiors and parameters of stars. This target is notable more for the extensive characterization of the host star rather than the discovered planet; the properties of astroseismic host stars can reveal both behaviors unique to hosts and properties that directly affect their exoplanets. HD 221416 also represents a star that has extensively evolved off the main sequence, possibly with its planet. These systems are useful for determining long-term planetary evolution with a variable host star.

High-Amplitude Outliers

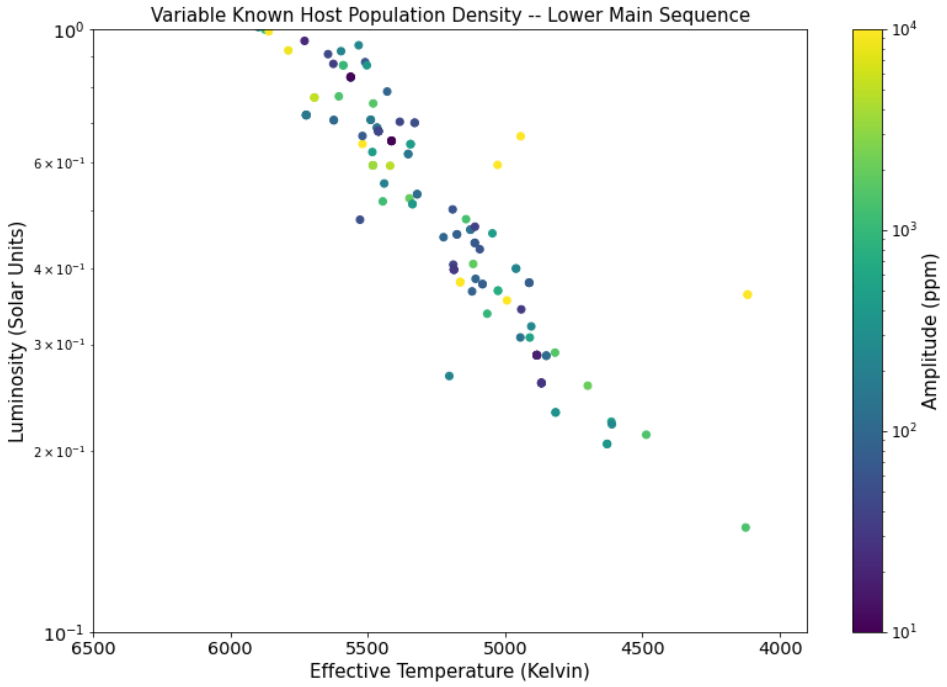

Figure 3.6 The lower main sequence portion of the HR diagram from Figure 3.2. The term "high-amplitude outliers" refers to targets in yellow.

There are targets within the lower main sequence that have high-amplitude variability. We chose targets with effective temperatures between 6200K and 3900K and luminosities between 0.1 and 1 solar luminosities, then made a cutoff of 7000 ppm photometric variability amplitude. This excluded the rest of the main sequence, along with the red giant branch. To understand how this compares to the whole population, we refer back to the initial variability analysis.

Analysis of the all-sky variable population revealed that the majority of high-amplitude targets within the main sequence were 2-peak and ACF targets, rather than

1-peak targets. When isolating the all-sky 1-peak solution targets within the HR diagram, it becomes visually similar to the left plot of Figure 3.2. This could be attributed to the majority of 1-peak solutions within the known host population, making up 86.1% of all known host targets (368 out of 427). A LS periodogram analysis of these ACF targets did not reveal unexpected behaviors for these stars in this section of the main sequence. These targets, according to Figure 3.5 were mostly detected via direct imaging. This explains the source of their variability: stars observed with direct imaging are young, and therefore more variable and active by nature.

These outliers reveal that there is a definitive correlation between the type of variability solution and the variability amplitude of these host stars. This could determine which types of stellar variability could be more prevalent in certain portions of the main sequence, and then change how stellar activity is accounted for photometric and spectroscopic data.

3.4 Discussion

3.4.1 The TICv8 Catalog

Upon first glance, these targets more or less lie within the expected range of stellar types. Most lie within the main sequence, but some populate the giant branches, as well as the low-mass branch on the lower right. The red giant branch is heavily populated, an expected outcome due to the focus group being variable stars. These giants tend to have excessive variability compared to other stellar types, usually a result of age. Some targets populate the very bottom of the sub-giant branch, but to not exceed this boundary. O- and

B-type stars are rare, and therefore not well-represented in any photometric mission as of current. In addition, exoplanets are not expected to be found orbiting these stars due to the extreme mass ratio (in the case of the RV method) and brightness (in regards to the transit method). Planets that might exist around these stars would be short-lived due to the short lifespan of these stars. An example of a blue giant host star that made it through will be elaborated upon further.

It was at this point where a glaring issue was revealed: the pulled TIC catalog values for these targets did not compare well to their published value counterparts on the NASA Exoplanet Archive. This was discovered when I identified targets within the HR diagram by their detection methods. An analysis of their parameters confirmed that the reported radii values for these stars differed from their published findings. Some were only minutely different, while others far exceeded their published counterparts.

Figure 3.7 demonstrates the movement of target parameters between each catalog. Some targets move more than others, with targets in the giant branch moving more than those within the main sequence. Additional uncertainty can also come from radius and effective temperature due to the presence of stellar variability. Those unconnected by lines do not have a counterpart in the other catalog.

This led to an investigation of why the TICv8 catalog values were incorrect. The reported stellar properties within the NASA Exoplanet Archive were much more accurate than the values pulled directly from the TICv8 catalog itself. The TICv8 publication describes the methods utilized to calculate these values. Effective temperature for these stars is taken from either spectroscopy or dereddened colors; whether this presents a biased dis-

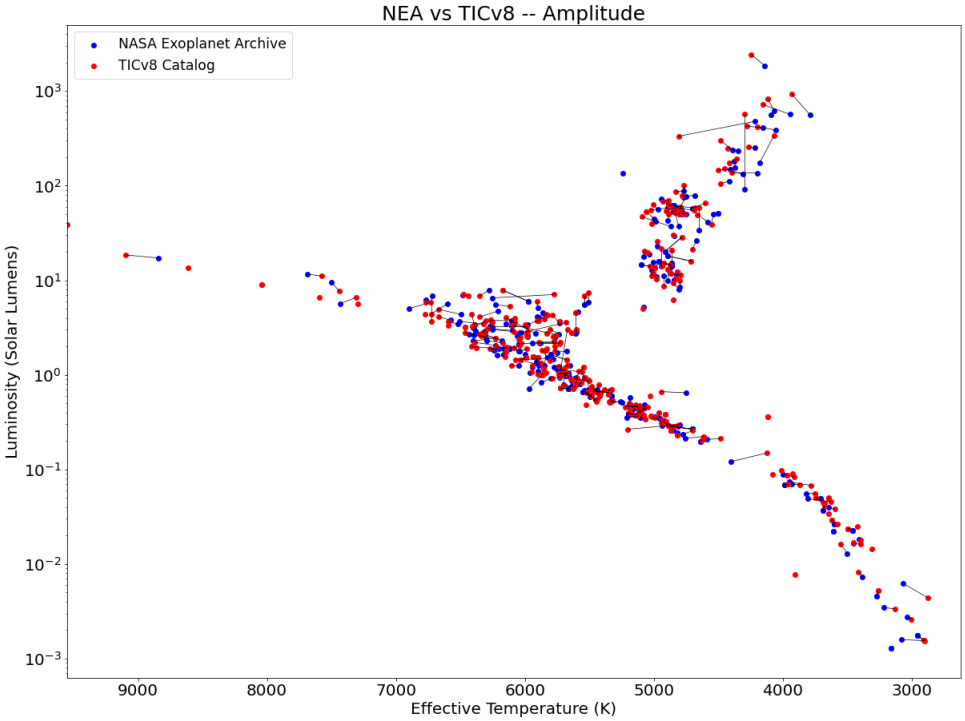

Figure 3.7 An HR diagram displaying the known host targets as they exists within the TICv8 and NASA Exoplanet Archive catalogs. Each target is connected to its counterpart with a black line. Note the larger gaps in luminosity values (aka reported vs. calculated radius values) for targets in either giant branch compared to the main sequence.

crepancy based on the color of the star remains to be seen. For stellar radii, the TICv8 value is calculated using the below Stefan-Boltzmann equation:

$$\mathbf{log(R/R_{\odot}) = \frac{1}{5}[4.74 - 5 + 5logD - G - 10log(T_{eff}/5772) - BC_G} \tag{3.1}$$

where D is the distance based on the Gaia parallax from (Gaia Collaboration et al. 2016), G is the observed Gaia magnitude corrected for extinction ($G_{obs} - A_G$). Effective temperatures from spectroscopy had 100K added in quadrature to the reported uncertainty if the Gaia

catalog reported less than 100K. It is speculated that the Stefan-Boltzmann law fails to an extent for giant stars, leading to an increase in error as the values stray away from the main sequence.

If the reported TICv8 values attributed to the NASA Exoplanet Archive page are correct, but the values directly imported from the TICv8 catalog are much more erroneous, there must be a discrepancy between the two. The source of these differences cannot be pinpointed via this study, but must be taken into consideration due to the stellar parameters being such a fundamental part of this work.

3.5 Conclusions

This analysis of known hosts observed by TESS has revealed critical information about this population of stars. By utilizing photometry from the TESS satellite, we see that variable known hosts populate a range of spectral types but vary in strength and variability classification in certain sub-regions. Exoplanets orbiting variable stars exist at a range of distances and compositions, from habitable-zone terrestrial to ultra-hot Jupiters and even with highly-eccentric orbits. Outliers within the stellar analysis allows for an in-depth look at how unique systems can form even with less stable stars and circumbinary systems. This study has the potential to provide a foundation of understanding that can be applied to both current variable planetary systems and those found in future exoplanet missions.

Chapter 4

Future Work

This study has focused on how variable host stars both affect how we perceive their planets, as well as how they determine the physical parameters of these planets. The struggle with observational biases when detecting planets around variable stars must be addressed. I intend to broaden and refine these findings in future works, as well as applying these analyses to new photometry missions to see how improved technology affects current observational biases. The potential to find more false positives lies with the success of upcoming missions. The star-planet connection has been recently highlighted as high-priority by the 2020 Decadal Survey. It is my hope that this work on the stellar variability of known hosts will contribute to the foundation of how the exoplanet community understands the star-planet connection.

Bibliography

Aigrain, S., Pont, F., & Zucker, S. 2012, MNRAS, 419, 3147, doi: 10.1111/j.1365-2966.2011.19960.x

Alonso, R., Brown, T. M., Torres, G., et al. 2004, ApJ, 613, L153, doi: 10.1086/425256

Bakos, G. Á., Noyes, R. W., Kovács, G., et al. 2007, ApJ, 656, 552, doi: 10.1086/509874

Black, D. C. 1980, Space Sci. Rev., 25, 35, doi: 10.1007/BF00200797

Boisse, I., Bouchy, F., Hébrard, G., et al. 2011, A&A, 528, A4, doi: 10.1051/0004-6361/201014354

Boro Saikia, S., Marvin, C. J., Jeffers, S. V., et al. 2018, A&A, 616, A108, doi: 10.1051/0004-6361/201629518

Borucki, W. J. 2016, Reports on Progress in Physics, 79, 036901, doi: 10.1088/0034-4885/79/3/036901

Borucki, W. J., Koch, D., Basri, G., et al. 2010, Science, 327, 977, doi: 10.1126/science.1185402

Bracewell, R. N., & MacPhie, R. H. 1979, Icarus, 38, 136, doi: 10.1016/0019-1035(79)90093-9

Butler, R. P., Wright, J. T., Marcy, G. W., et al. 2006, ApJ, 646, 505, doi: 10.1086/504701

Crane, J. D., Shectman, S. A., Butler, R. P., et al. 2010, in Society of Photo-Optical Instrumentation Engineers (SPIE) Conference Series, Vol. 7735, Ground-based and Airborne Instrumentation for Astronomy III, ed. I. S. McLean, S. K. Ramsay, & H. Takami, 773553, doi: 10.1117/12.857792

Delisle, J. B., Hara, N., & Ségransan, D. 2020, A&A, 635, A83, doi: 10.1051/0004-6361/201936905

Desort, M., Lagrange, A. M., Galland, F., Udry, S., & Mayor, M. 2007, A&A, 473, 983, doi: 10.1051/0004-6361:20078144

Díaz, M. R., Jenkins, J. S., Tuomi, M., et al. 2018, AJ, 155, 126, doi: 10.3847/1538-3881/aaa896

Dragomir, D., Kane, S. R., Henry, G. W., et al. 2012, ApJ, 754, 37, doi: 10.1088/0004-637X/754/1/37

Dreizler, S., Jeffers, S. V., Rodríguez, E., et al. 2020, MNRAS, 493, 536, doi: 10.1093/mnras/staa248

Fischer, D. A., Anglada-Escude, G., Arriagada, P., et al. 2016, PASP, 128, 066001, doi: 10.1088/1538-3873/128/964/066001

Fulton, B. J., Petigura, E. A., Blunt, S., & Sinukoff, E. 2018, PASP, 130, 044504, doi: 10.1088/1538-3873/aaaaa8

Fulton, B. J., Petigura, E. A., Howard, A. W., et al. 2017, AJ, 154, 109, doi: 10.3847/1538-3881/aa80eb

Gaia Collaboration, Prusti, T., de Bruijne, J. H. J., et al. 2016, A&A, 595, A1, doi: 10.1051/0004-6361/201629272

Gaia Collaboration, Brown, A. G. A., Vallenari, A., et al. 2018, A&A, 616, A1, doi: 10.1051/0004-6361/201833051

—. 2021, A&A, 649, A1, doi: 10.1051/0004-6361/202039657

Gardner, J. P., Mather, J. C., Clampin, M., et al. 2006, Space Sci. Rev., 123, 485, doi: 10.1007/s11214-006-8315-7

Gaudi, B. S., Stassun, K. G., Collins, K. A., et al. 2017, Nature, 546, 514, doi: 10.1038/nature22392

Gillon, M., Demory, B. O., Lovis, C., et al. 2017, A&A, 601, A117, doi: 10.1051/0004-6361/201629270

Guerrero, N. M., Seager, S., Huang, C. X., et al. 2021, ApJS, 254, 39, doi: 10.3847/1538-4365/abefe1

Hawley, S. L., Gizis, J. E., & Reid, I. N. 1996, AJ, 112, 2799, doi: 10.1086/118222

Heng, K., & Showman, A. P. 2015, Annual Review of Earth and Planetary Sciences, 43, 509, doi: 10.1146/annurev-earth-060614-105146

Henry, G. W., Donahue, R. A., & Baliunas, S. L. 2002, ApJ, 577, L111, doi: 10.1086/344291

Howell, S. B., Sobeck, C., Haas, M., et al. 2014, PASP, 126, 398, doi: 10.1086/676406

Huber, D., Chaplin, W. J., Chontos, A., et al. 2019, AJ, 157, 245, doi: 10.3847/1538-3881/ab1488

Jenkins, J. M., Twicken, J. D., McCauliff, S., et al. 2016, in Society of Photo-Optical Instrumentation Engineers (SPIE) Conference Series, Vol. 9913, Software and Cyberinfrastructure for Astronomy IV, ed. G. Chiozzi & J. C. Guzman, 99133E, doi: 10.1117/12.2233418

Kane, S. R., Mahadevan, S., von Braun, K., Laughlin, G., & Ciardi, D. R. 2009, PASP, 121, 1386, doi: 10.1086/648564

Kane, S. R., Clarkson, W. I., West, R. G., et al. 2008, MNRAS, 384, 1097, doi: 10.1111/j.1365-2966.2007.12722.x

Kane, S. R., Dragomir, D., Ciardi, D. R., et al. 2011, ApJ, 737, 58, doi: 10.1088/0004-637X/737/2/58

Kane, S. R., Thirumalachari, B., Henry, G. W., et al. 2016, ApJ, 820, L5, doi: 10.3847/2041-8205/820/1/L5

Kane, S. R., Bean, J. L., Campante, T. L., et al. 2021, PASP, 133, 014402, doi: 10.1088/1538-3873/abc610

Kenknight, C. E. 1977, Icarus, 30, 422, doi: 10.1016/0019-1035(77)90176-2

Konacki, M., Torres, G., Jha, S., & Sasselov, D. D. 2003, Nature, 421, 507, doi: 10.1038/nature01379

Kopparapu, R. K., Ramirez, R. M., SchottelKotte, J., et al. 2014, ApJ, 787, L29, doi: 10.1088/2041-8205/787/2/L29

Kopparapu, R. K., Ramirez, R., Kasting, J. F., et al. 2013, ApJ, 765, 131, doi: 10.1088/0004-637X/765/2/131

Lammer, H., Lichtenegger, H. I. M., Kulikov, Y. N., et al. 2007, Astrobiology, 7, 185, doi: 10.1089/ast.2006.0128

Lo Curto, G., Mayor, M., Benz, W., et al. 2013, A&A, 551, A59, doi: 10.1051/0004-6361/201220415

Lomb, N. R. 1976, Ap&SS, 39, 447, doi: 10.1007/BF00648343

Mayor, M., & Queloz, D. 1995, Nature, 378, 355, doi: 10.1038/378355a0

Mayor, M., Pepe, F., Queloz, D., et al. 2003, The Messenger, 114, 20

McQuillan, A., Aigrain, S., & Roberts, S. 2012, A&A, 539, A137, doi: 10.1051/0004-6361/201016148

Morales, J. C., Mustill, A. J., Ribas, I., et al. 2019, Science, 365, 1441, doi: 10.1126/science.aax3198

NASA Exoplanet Archive. 2021, Planetary Systems, Version: 2021-12-18, NExScI-Caltech/IPAC, doi: 10.26133/NEA12

Nava, C., López-Morales, M., Haywood, R. D., & Giles, H. A. C. 2020, AJ, 159, 23, doi: 10.3847/1538-3881/ab53ec

Pepe, F., Mayor, M., Delabre, B., et al. 2000, in Society of Photo-Optical Instrumentation Engineers (SPIE) Conference Series, Vol. 4008, Optical and IR Telescope Instrumentation and Detectors, ed. M. Iye & A. F. Moorwood, 582–592, doi: 10.1117/12.395516

Ribas, I., Guinan, E. F., Güdel, M., & Audard, M. 2005, ApJ, 622, 680, doi: 10.1086/427977

Ricker, G. R., Winn, J. N., Vanderspek, R., et al. 2015, Journal of Astronomical Telescopes, Instruments, and Systems, 1, 014003, doi: 10.1117/1.JATIS.1.1.014003

Robertson, P., Endl, M., Henry, G. W., et al. 2015, ApJ, 801, 79, doi: 10.1088/0004-637X/801/2/79

Robertson, P., & Mahadevan, S. 2014, ApJ, 793, L24, doi: 10.1088/2041-8205/793/2/L24

Rodríguez-Mozos, J. M., & Moya, A. 2019, A&A, 630, A52, doi: 10.1051/0004-6361/201935543

Rosenthal, L. J., Fulton, B. J., Hirsch, L. A., et al. 2021, ApJS, 255, 8, doi: 10.3847/1538-4365/abe23c

Saar, S. H., & Donahue, R. A. 1997, ApJ, 485, 319, doi: 10.1086/304392

Scargle, J. D. 1982, ApJ, 263, 835, doi: 10.1086/160554

Schneider, J., Dedieu, C., Le Sidaner, P., Savalle, R., & Zolotukhin, I. 2011, A&A, 532, A79, doi: 10.1051/0004-6361/201116713

Seager, S., & Mallén-Ornelas, G. 2003, ApJ, 585, 1038, doi: 10.1086/346105

Segura, A., Walkowicz, L. M., Meadows, V., Kasting, J., & Hawley, S. 2010, Astrobiology, 10, 751, doi: 10.1089/ast.2009.0376

Showman, A. P., Fortney, J. J., Lewis, N. K., & Shabram, M. 2013, ApJ, 762, 24, doi: 10.1088/0004-637X/762/1/24

Shporer, A. 2017, PASP, 129, 072001, doi: 10.1088/1538-3873/aa7112

Stassun, K. G., Oelkers, R. J., Paegert, M., et al. 2019, AJ, 158, 138, doi: 10.3847/1538-3881/ab3467

Sulis, S., Mary, D., & Bigot, L. 2017, IEEE Transactions on Signal Processing, 65, 2136, doi: 10.1109/TSP.2017.2652391

Süveges, M. 2014, MNRAS, 440, 2099, doi: 10.1093/mnras/stu372

Trifonov, T., Tal-Or, L., Zechmeister, M., et al. 2020, A&A, 636, A74, doi: 10.1051/0004-6361/201936686

Tuomi, M. 2014, MNRAS, 440, L1, doi: 10.1093/mnrasl/slu014

van Belle, G. T., & von Braun, K. 2009, ApJ, 694, 1085, doi: 10.1088/0004-637X/694/2/1085

Vanderburg, A., Plavchan, P., Johnson, J. A., et al. 2016, MNRAS, 459, 3565, doi: 10.1093/mnras/stw863

Vio, R., & Andreani, P. 2016, A&A, 589, A20, doi: 10.1051/0004-6361/201527463

Vio, R., Andreani, P., Biggs, A., & Hayatsu, N. 2019, A&A, 627, A103, doi: 10.1051/0004-6361/201834854

Zechmeister, M., & Kürster, M. 2009, A&A, 496, 577, doi: 10.1051/0004-6361:200811296

Zechmeister, M., Reiners, A., Amado, P. J., et al. 2018, A&A, 609, A12, doi: 10.1051/0004-6361/201731483

Zellem, R. T., Swain, M. R., Roudier, G., et al. 2017, ApJ, 844, 27, doi: 10.3847/1538-4357/aa79f5

Zuckerman, B. 2015, in Astronomical Society of the Pacific Conference Series, Vol. 493, 19th European Workshop on White Dwarfs, ed. P. Dufour, P. Bergeron, & G. Fontaine, 291. https://arxiv.org/abs/1410.2575